25th ABCM International Congress of Mechanical Engineering
October 20-25, 2019, Uberlândia, MG, Brazil

COB-2019-0838

STUDY OF NON-ISOTHERMAL TWO-DIMENSIONAL FLOW OVER A SQUARE CYLINDER IMMERSED IN A CHANNEL

Gabriel Machado dos Santos
Ítalo Augusto Magalhães de Ávila
Hélio Ribeiro Neto
João Marcelo Vedovoto
Federal University of Uberlândia, Av. João Naves de Ávila 2121, Campus Santa Mônica. Uberlândia, MG, Brazil, CEP: 38400-902.
gabriel.msantos@ufu.br, italo.ufuracing@gmail.com, heliorine@hotmail.com, vedovoto@ufu.br

Abstract. *In the present paper, the mathematical and numerical-computational modeling of the non-isothermal flow over a square cylinder immersed in a channel is presented, in order to evaluate the influence of Reynolds number over the mass and energy transport phenomena. The mathematical model is based on the classic fluid mechanics equations. For the numerical model, the finite difference method and the fractional step method for the pressure-velocity coupling are employed. Computational routines are implemented and the results obtained are compared with those presented in the literature.*

Keywords: *computational fluid mechanics, numerical simulation, two-dimensional flow, non-isothermal flow, flow over a square cylinder*

1. INTRODUCTION

The study of flows over immersed bodies is of interest to a wide range of engineering practices. This fact is due to its high applicability in the improvement of industrial processes, besides making possible a better understanding of the natural phenomena. The investigation of this class of problems is usually carried out through material and virtual experiments. Virtual research, in this context, presents itself as a good alternative for the analysis of problems related to flows over solid geometries.

The flow over cylinders is a canonical problem, which was studied by a wide range of researchers as Okajima (1982), Kim *et al.* (2001) and Lima e Silva (2002). Although the geometry is simple, the modeling of such case can provide valuable information such as vortex shedding frequency, drag and lift coefficients, and thermal energy transport. The comparison of its solution with the ones found in the literature is fundamental for the validation of the developed numerical-computational model, which can later be implemented for complex geometries.

This work is based on the investigation of the flow through virtual experimentation. In this manner, the physical and mathematical modeling of the problem under analysis is essential. Physical modeling consists of a representation of the real phenomenon investigated, in which physical assumptions are considered, aiming the simplification of the observed phenomenon in order to make its analysis feasible. Mathematical modeling is the determination of mathematical equations that model the physics of the problem being analised, where such equations can be algebraic, differential, integral or integral-differential.

2. PHYSICAL AND MATHEMATICAL MODELING

For the present work, a square cylinder, whose surface is maintained at a constant temperature, is considered. This cylinder is immersed in a channel, where the imposed inlet velocity and temperature are uniform and the outlet is defined by the Neumann boundary condition for velocities and temperature. The horizontal walls admit Neumann conditions for temperature and the non-slip condition for velocities (Fig. 1a), as well as the cylinder faces (Fig.1b). The dimensions of the channel are based on the dimension of the edge of the square (D): $L_{bot} = 10D$, $L_{left} = 15D$, $L_{right} = 45D$ and $L_{top} = 10D$. For the present study, the flow is considered incompressible and the fluid is modeled as a Newtonian fluid.

The equations that model the energy transport and transformations in fluid flows are obtained through the analysis of a reference element volume (REV). Therefore, it is necessary to use the Reynolds Transport Theorem (RTT), Newton's second law and the first law of thermodynamics. Initially, when performing the mass flow balance in the REV, applying it to the ratio of mass conservation obtained through RTT, we obtain the continuity equation. Applying the hypothesis that the flow is incompressible, the continuity equation is then simplified:

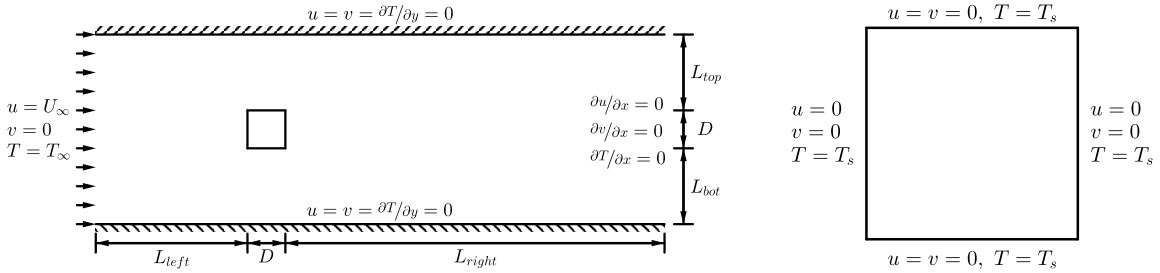

(a) Channel boundary conditions. (b) Immersed body boundary conditions.

Figure 1: Schematic representation of the problem addressed.

$$\boldsymbol{\nabla}\cdot\mathbf{V} = 0, \tag{1}$$

where $\mathbf{V}$ represents the velocity vector of the fluid element.

When Newton's second law is applied to the REV, one models that the acceleration of the element is proportional to the external forces acting upon it. In this study, only the force due to gravitational effects (modeled by the Boussinesq's approach) and the surface forces, due to the stresses on the surface of the element and originated from the pressure and the viscous stresses, will be considered. In this way, when one analyses the linear momentum deviation in a differential element, the stress tensor is modeled for a Newtonian fluid, the equations of the movement of the fluid are obtained:

$$\frac{\partial \mathbf{V}}{\partial t} + (\mathbf{V}\cdot\boldsymbol{\nabla})\,\mathbf{V} = -\frac{1}{\rho}\boldsymbol{\nabla} p - \beta(T - T_o)\mathbf{g} + \frac{\mu}{\rho}\boldsymbol{\nabla}^2\mathbf{V}, \tag{2}$$

where, $\mathbf{g}$ represents the gravitational field, p is the pressure, T the local temperature, T_o the reference temperature, ρ the specific mass of the fluid, μ represents its dynamic viscosity and β the coefficient of thermal expansion.

To obtain the equation that models the temperature field (by neglecting the effects of radiation), the Fourier's law is used to perform the thermal energy balance in the differential element and the tensor of viscous stress for the modeling of the work due the viscous forces, applying them in the balance equation of the energy obtained by RTT, one obtains the differential equation of the thermal energy:

$$\frac{\partial T}{\partial t} + (\mathbf{V}\cdot\boldsymbol{\nabla})\,T = \frac{k}{\rho c_p}\boldsymbol{\nabla}^2 T + \frac{1}{\rho c_p}\Phi, \tag{3}$$

where Φ is the viscous transformation function, k is the coefficient of thermal conductivity of the fluid and c_p represents its thermal capacity.

The characterization of the flow can be defined through some dimensionless numbers such as the Reynolds number (Re) which is related to the ratio between the inertial and viscous effects, the Strouhal number (St) which is the dimensionless vortex shedding frequency, the Prandtl number (Pr) which relates the linear momentum and thermal diffusivity, the Grashof number (Gr) which correlates the gravitational force and the viscous forces, and the Nusselt number (Nu) which confronts the transfer of thermal energy by advection and diffusion.

$$Re = \frac{\rho U_\infty D}{\mu}, \tag{4}$$

$$St = \frac{fD}{U_\infty}, \tag{5}$$

$$Pr = \frac{c_p \mu}{k}, \tag{6}$$

$$Gr = \frac{g\rho^2\beta(T_s - T_\infty)D^3}{\mu^2}, \tag{7}$$

$$\theta = \frac{T_s - T}{T_s - T_\infty}, \tag{8}$$

$$Nu = D\left.\frac{\partial\theta}{\partial y}\right|_{y=\text{wall}}, \tag{9}$$

where f is the vortex shedding frequency, θ is the dimensionless temperature, U_∞ and T_∞ are the velocity and temperature of the channel inlet flow, respectively.

3. NUMERICAL-COMPUTATIONAL MODELING

Once the physical and mathematical models have been defined, one might develop a numerical-computational model. This type of modeling is employed with the purpose of obtaining approximate solutions to the equations obtained in the mathematical model. For such, the domain discretization is necessary, process in which a continuous set of information is translated into a discrete one. This way the domain is partitioned uniformly by generating the mesh $\mathcal{M}$:

$$\mathcal{M} = \{(t^n, x_i, y_j)\,;\; t^n = n\Delta t,\; x_i = i\Delta x,\; y_j = j\Delta y,\; n = 0, 1, \ldots, K,\; i = 0, 1, \ldots, L,\; j = 0, 1, \ldots, M\}\,. \tag{10}$$

where Δt is the time step, Δx and Δy are the spatial steps in the horizontal and vertical directions, respectively. The superscript n refers to temporal discretization, and similarly subindices i and j refer to spatial discretization in their respective directions.

For the solution of the equations that model the fluid dynamics (Eq. 1 and Eq. 2), the fractional step methodology is employed (Kim and Moin, 1985). In this method, for a explicit discretization, the velocity components are estimated by solving the linear momentum equations using the velocity and pressure fields at the previous time step. The pressure in the current time step is modeled as the sum of the pressure in the previous time step, plus a correction factor (Eq. 13), which is calculated using a Poisson equation (Eq. 12) obtained by combining the linear momentum and continuity equations. The current velocity field is then corrected with the pressure correction factor, so that the continuity equation is satisfied (Eq. 14). In this manner, the following system of equations is obtained:

$$\frac{\hat{\mathbf{V}} - \mathbf{V}^n}{\Delta t} = -\frac{1}{\rho}\boldsymbol{\nabla} p^n - \beta(T - T_o)\mathbf{g}^n - (\mathbf{V}^n \cdot \boldsymbol{\nabla})\,\mathbf{V}^n + \frac{\mu}{\rho}\boldsymbol{\nabla}^2\mathbf{V}^n, \tag{11}$$

$$\boldsymbol{\nabla}^2 p' = \frac{\rho}{\Delta t}\,\boldsymbol{\nabla} \cdot \hat{\mathbf{V}}, \tag{12}$$

$$p^{n+1} = p^n + p', \tag{13}$$

$$\mathbf{V}^{n+1} = \hat{\mathbf{V}} - \frac{\Delta t}{\rho}\boldsymbol{\nabla} p', \tag{14}$$

where $\hat{\mathbf{V}}$ is the estimated velocity field, p' is the pressure correction factor and the superscript n represents the time step of temporal discretization.

Figure 2 is a flowchart of the procedure performed for the prediction of velocity and pressure fields at the next time step, applying the fractional step method for an explicit time discretization.

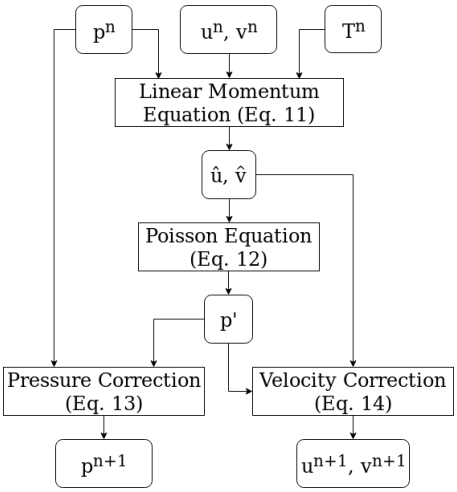

Figure 2: Method flowchart.

The system of equations mentioned above, as well as the thermal energy equation (Eq. 3), must then be discretized. For that, the finite difference method with staggered mesh is used, where the velocities are located in the faces and pressure and temperature in the center of the computational cell, as shown in Fig. 3.

The Central Difference Scheme (CDS) is used for the spatial derivatives, while explicit Euler scheme is applied on the time derivative. The linear system obtained on the discrete Poisson equation is solved by the biconjugate gradient stabilized method (Van der Vorst, 1992).

The discretized equations are then implemented in computational routines using the Fortran 90 programming language. Particular cases are implemented and the computational results are compared with the literature, in order to validate the in-house developed code.

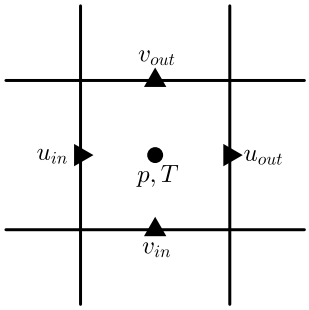

Figure 3: Representation of displaced meshes.

4. VALIDATION

Five simulations are performed and the results for different flow regimes are compared to those presented in the literature. The first simulation is performed for $Re = 30$ and $Pr = 0.71$, in order to qualitatively compare the streamlines with those presented by Breuer *et al.* (2000). The results are presented in Fig. 4.

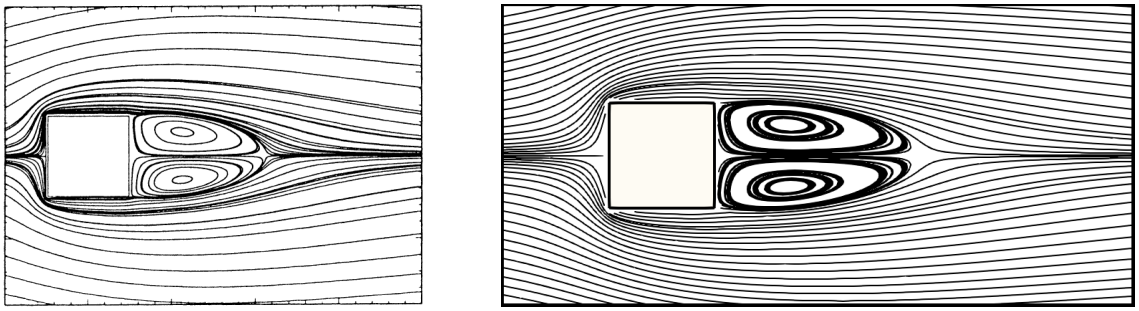

(a) Breuer *et al.* (2000) (b) Present work

Figure 4: Streamlines over the cylinder for $Re = 30$ and $Pr = 0.71$.

The second simulation was performed in the condition of $Re = 40$ and $Pr = 10$, in order to determine recirculation length formed downstream of the cylinder to its edge. Such ratio was determined as 2.575, resulting in a percentual error of 4.65% when compared to the work of Paliwal *et al.* (2003). The third case was simulated with $Re = 100$ and $Pr = 0.71$, regime in which vortex shedding phenomena can be observed. Thus, the Strouhal number was calculated from the oscillations in the vertical velocity component at a point of the domain located in the line of axial symmetry of the channel and at $L = 22.5D$ to the right of the cylinder (Fig. 5), the value obtained was 0.152, which presents a deviation of 4.83% from the results presented by Ma *et al.* (2018).

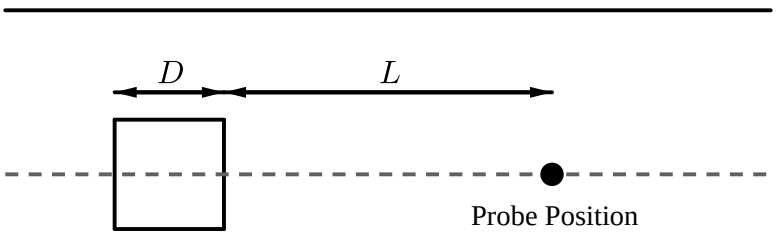

Figure 5: Schematic representation of the probe position in the domain.

The remaining simulations were carried out with the purpose of evaluating the methodology applied to thermal modeling. Thus, the local Nusselt number along the cylinder faces is calculated for two flow regimes ($Re = 1$ and $Re = 45$, both with $Pr = 1$), the results are in accord with those presented by Dhiman *et al.* (2006) as can be observed in Fig. 6.

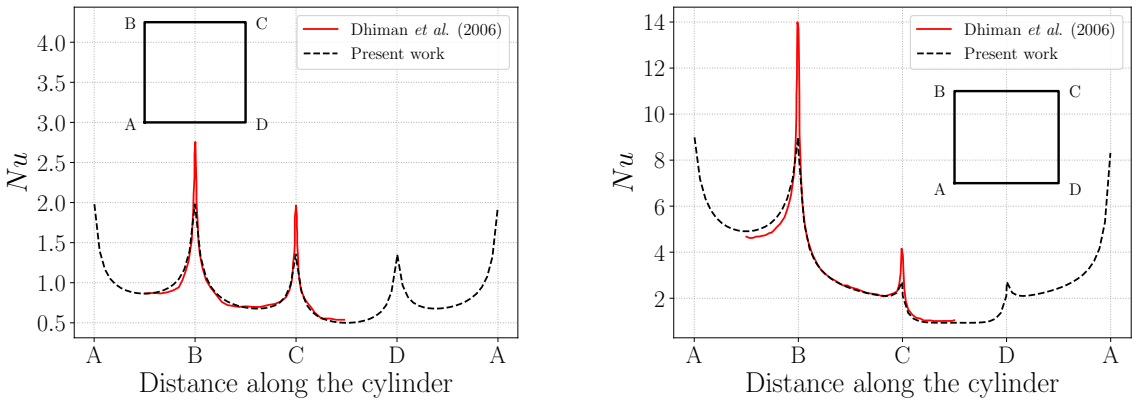

(a) $Re = 1$ e $Pr = 1$.

(b) $Re = 45$ e $Pr = 1$.

Figure 6: Local Nusselt number along the sides of the cylinder.

5. RESULTS

In order to evaluate the influence of the Reynolds number over the transport phenomena on two-dimensional flow around a heated square cylinder, computational simulations are conducted for fixed values of Prandtl and Grashof numbers ($Pr = 0.71$ e $Gr = 0$) and the Reynolds number values of 100, 150, and 200.

The boundary conditions are presented in Fig. 1, which shows that, for the present work, the constant temperature situation on the surface of the immersed geometry ($\theta = 1$) is modeled. For the simulations conducted, an uniform and regular mesh of 1220×420 is adopted, which sets an uniform spatial step of 2.5 mm. The computational results of the vorticity and temperature fields are presented in Fig. 7 and Fig. 8, respectively.

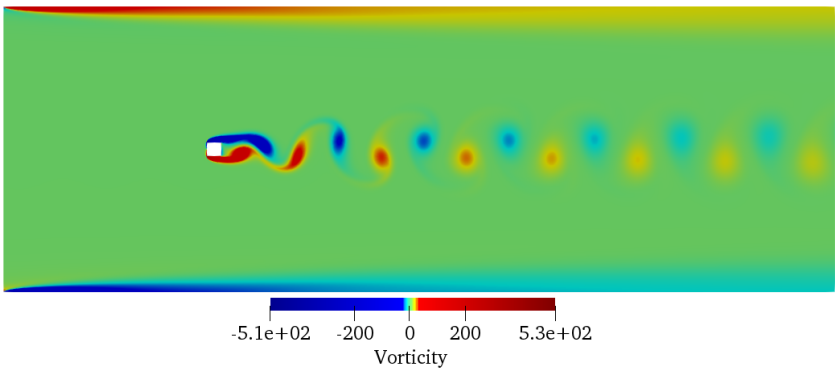

(a) $Re = 100$ and $\tau = 620$.

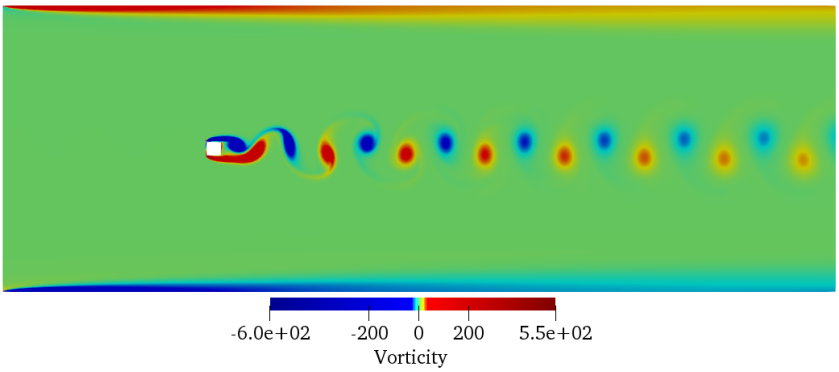

(b) $Re = 150$ and $\tau = 572$.

Figure 7: Vorticity field for different Reynolds number values and $Pr = 0.71$.

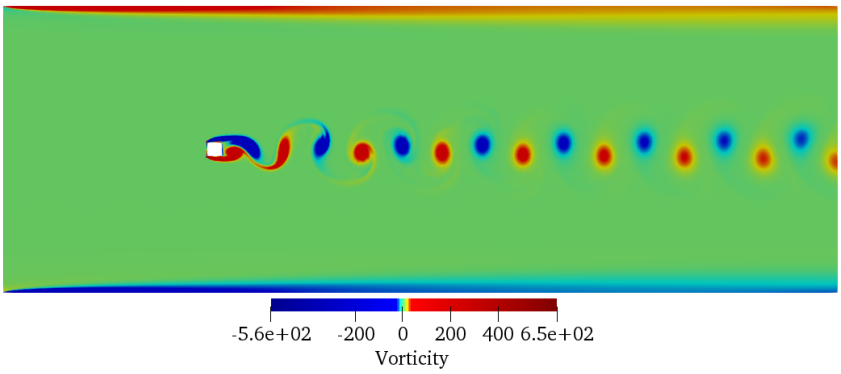

(c) $Re = 200$.

Figure 7: Vorticity field for different Reynolds number values and $Pr = 0.71$.

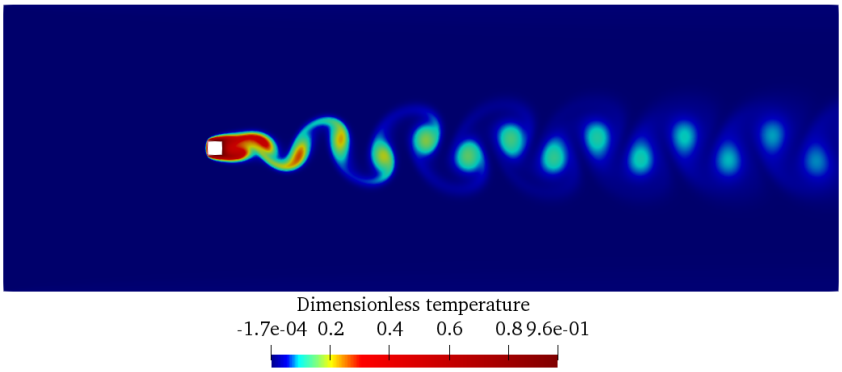

(a) $Re = 100$ and $\tau = 620$.

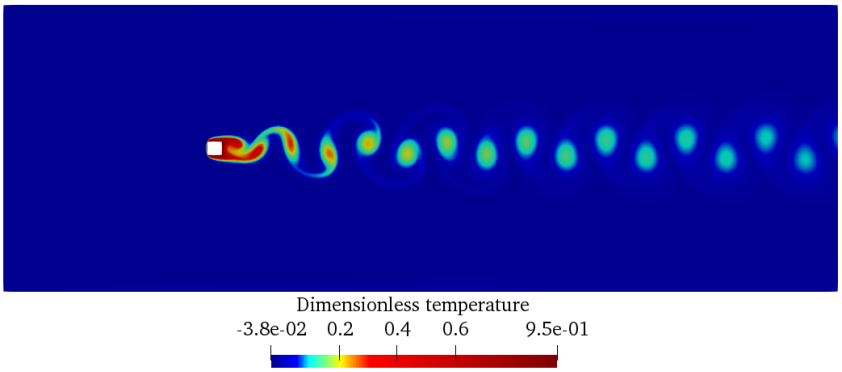

(b) $Re = 150$ and $\tau = 572$.

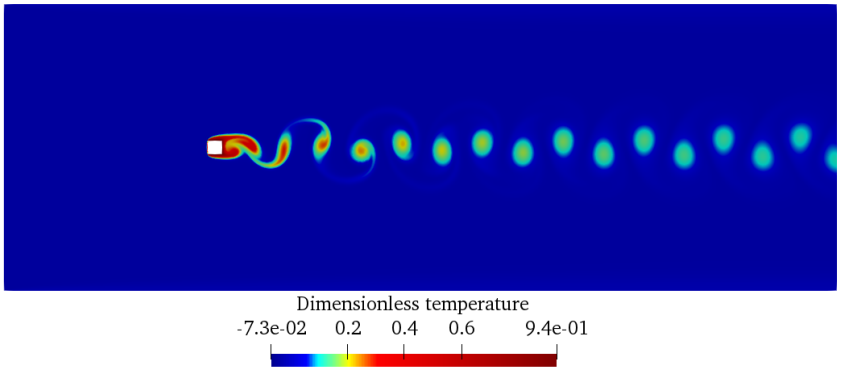

(c) $Re = 200$ and $\tau = 302$.

Figure 8: Temperature field for different Reynolds number values and $Pr = 0.71$.

The computational results presented in Fig. 7 show the scalar vorticity field, a variable that quantifies the rotation intensity of the particles contained in the evaluated element. It is possible to observe, downstream the cylinder, the formation of von Kármán vortex streets, characterized by the symmetrical and regular vortex emission. Note that higher vorticity values are related to higher Reynolds values. The justification of this relationship is due to the fact that the equations that model the mechanics of fluids constitute a dynamic system of unstable character, and higher values of the dimensionless, or larger proportions of advective effects in relation to diffusive effects, are pertinent for the amplification and transport of instabilities to the detriment of diffusion mechanisms.

According to the above interpretation, higher dimensionless values are also expected to be associated with higher vortex emission rates. The hypothesis is confirmed according to Tab. 1, which presents the relation between Strouhal number, dimensionless vortex shedding frequency, and Reynolds number.

Table 1: Strouhal number for different Reynolds number values and $Pr = 0.71$.

Reynolds number	100	150	200
Strouhal number	0.1539	0.1669	0.1726

The temperature field is presented at Fig. 8. Regarding the transport of thermal energy, it is observed that the increase in the value of the Reynolds number impacts substantialy the advective effects, in a similar maner to that observed for the transport of linear momentum. The increase in the proportion of inertial effects is evidenced by the higher concentration of thermal energy in the structures formed downstream the obstacle. For higher dimensionless values, the energy is transported by particles passing through the cylinder's periphery and accompanying them for a significant time, since diffusive transport phenomena are not efficient enough to transport energy from the vortices to adjacent regions.

Also, the drag and lift coefficients were calculated for each of the simulations, the results are presented in Fig. 9 and Tab. 2. Initially, it is observed that the dimensionless time ($\tau = tU_\infty/D$), in which the formation and detachment of the vortices begins, decreases due to the increase of the Reynolds number, evidencing the influence of the inertial effects over the amplification and transport of flow instabilities. It is also noted that there is a considerable increase in the amplitude of oscillation of the lift coefficient, this fact is due to the formation of larger velocity gradients and, consequently, larger pressure gradients.

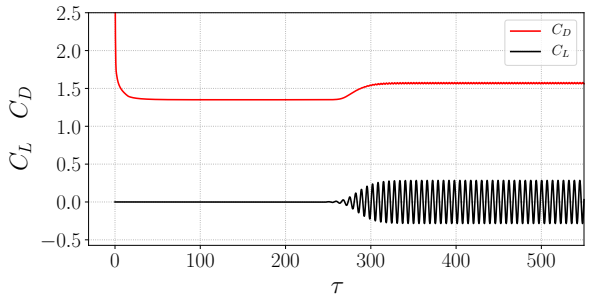

(a) $Re = 100$.

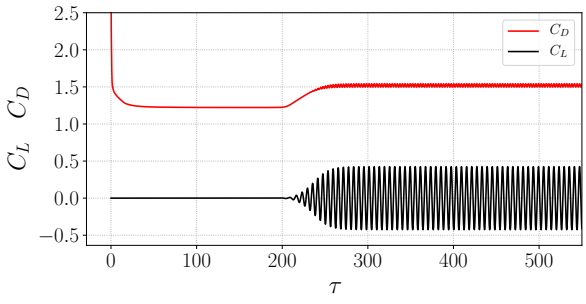

(b) $Re = 150$.

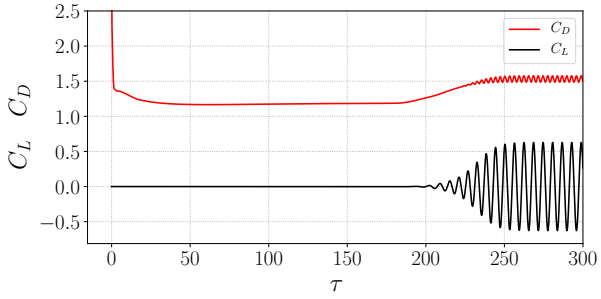

(c) $Re = 200$.

Figure 9: Drag and lift coefficients for different Reynolds number values.

Finally, Fig. 10 shows the profile of the local Nusselt number along the cylinder faces as a function of the Reynolds number. Larger Reynolds imply an increase in the local Nusselt number, which is expected, once the Nusselt number represents the capacity for convective thermal energy transfer. Thus, the greater the proportion of inertial effects on flow, the more efficient convection transport is. The average values of the Nusselt number are presented in Tab. 3, where we

Table 2: Drag and lift coefficients for different Reynolds values

Reynolds number	100	150	200
Average drag coefficient	1.5697	1.5200	1.5308
RMS lift coefficient	0.2016	0.3009	0.4405

notice that in fact, Nusselt increases with Reynolds.

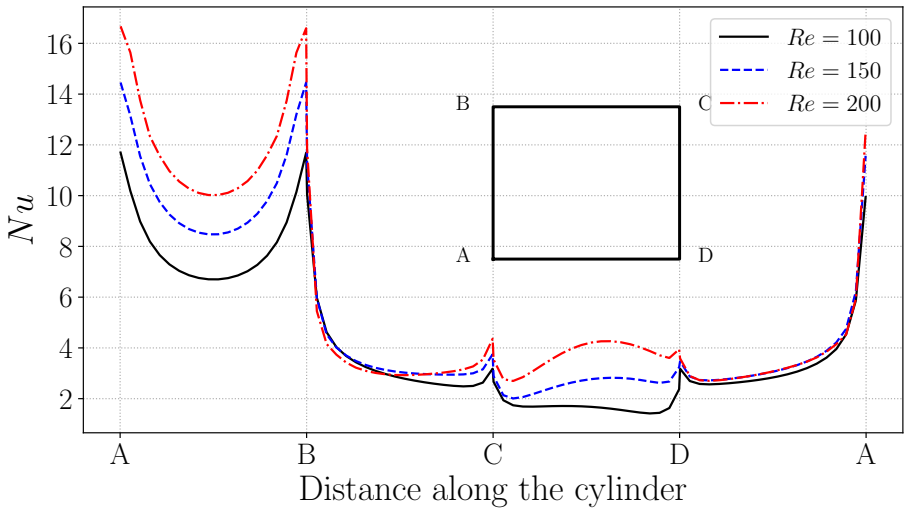

Figure 10: Local Nusselt number along the sides of the cylinder for different Reynolds numbers.

Table 3: Average Nusselt number value on cylinder surfaces for different Reynolds values and $Pr = 0.71$.

Reynolds number	100	150	200
Average Nusselt number	4.2265	5.1420	5.8837

6. CONCLUSION

In the present work, the physical, mathematical and numerical-computational modeling of non-isothermal flows over a square-shaped cylinder was presented. The results obtained with the developed computational code are compared with those encountered in the literature. The small deviations between them indicate a correct modeling of the transport phenomena present in the proposed problem.

Simulations were performed to analyze the influence of the Reynolds number over the flow dynamics and the thermal energy transport. The results show that the Reynolds number is directly related to the formation and detachment of vortices downstream the obstacle, as well as the drag and lift coefficient values. In addition, the Reynolds number also have influence on the value of the local Nusselt number on the faces of the heated cylinder.

7. ACKNOWLEDGEMENTS

The authors would like to thank Petrobras, CAPES, FAPEMIG, CNPq, MFLab and PROPP-UFU and specially the teacher Dr. Aristeu da Silveira Neto for the coorientation and support in the development of this work.

8. REFERENCES

Breuer, M., Bernsdorf, J., Zeiser, T. and Durst, F., 2000. “Accurate computations of the laminar flow past a square cylinder based on two diferent methods: lattice-boltzmann and finite-volume”. *International Journal of Heat and Fluid Flow*, Vol. 21, pp. 186–196.

Dhiman, A.K., Chhabra, R.P., Sharma, A. and Eswarani, V., 2006. “Effects of reynolds and prandtl numbers on heat

transfer across a square cylinder in the steady flow regime". *Numerical Heat Transfer, Part A: Applications: An International Journal of Computation and Methodology*, Vol. 49, No. 7, pp. 717–731.

Kim, J. and Moin, P., 1985. "Application of a fractional-step method to incompressible navier-stokes equations". *Journal of Computational Physics*, Vol. 59, pp. 308–323.

Kim, J., Kim, D. and Choi, H., 2001. "An immersed-boundary finite-volume method for simulations of flow in complex geometries". *Journal of Computational Physics*, Vol. 171, pp. 132–150.

Lima e Silva, A.L.F., 2002. "Desenvolvimento e implementação de uma nova metodologia para modelagem de escoamentos sobre geometrias complexas: Método da fronteira imersa com modelo físico virtual".

Ma, Y., Mohebbi, R., Rashidi, M.M. and Yang, Z., 2018. "Numerical simulation of flow over a square cylinder with upstream and downstream circular bar using lattice boltzmann method". *International Journal of Modern Physics C*, Vol. 29, No. 4, pp. 1–28.

Okajima, A., 1982. "Strouhal numbers of rectangular cylinders". *Journal of Fluid Mechanics*, Vol. 123, pp. 379–398.

Paliwal, B., Sharma, A., Chhabra, R.P. and Eswaran, V., 2003. "Power law fluid flow past a square cylinder: Momentum and heat transfer characteristics". *Chemical Engineering Science*, Vol. 58, pp. 5315–5329.

Van der Vorst, H.A., 1992. "Bi-CGSTAB: A fast and smoothly converging variant of Bi-CG for the solution of nonsymmetric linear systems". *SIAM Journal on Scientific and Statistical Computing*, Vol. 13, No. 2, pp. 631–644.

9. RESPONSIBILITY NOTICE

The authors are the only responsible for the printed material included in this paper.